Bio-inspired self-healing structural color hydrogel

Fanfan Fu[a,1], Zhuoyue Chen[a,1], Ze Zhao[a], Huan Wang[a], Luoran Shang[a], Zhongze Gu[a], and Yuanjin Zhao[a,2]

[a]State Key Laboratory of Bioelectronics, School of Biological Science and Medical Engineering, Southeast University, Nanjing 210096, China

Edited by David A. Weitz, Harvard University, Cambridge, MA, and approved April 24, 2017 (received for review March 3, 2017)

Biologically inspired self-healing structural color hydrogels were developed by adding a glucose oxidase (GOX)- and catalase (CAT)-filled glutaraldehyde cross-linked BSA hydrogel into methacrylated gelatin (GelMA) inverse opal scaffolds. The composite hydrogel materials with the polymerized GelMA scaffold could maintain the stability of an inverse opal structure and its resultant structural colors, whereas the protein hydrogel filler could impart self-healing capability through the reversible covalent attachment of glutaraldehyde to lysine residues of BSA and enzyme additives. A series of unprecedented structural color materials could be created by assembling and healing the elements of the composite hydrogel. In addition, as both the GelMA and the protein hydrogels were derived from organisms, the composite materials presented high biocompatibility and plasticity. These features of self-healing structural color hydrogels make them excellent functional materials for different applications.

colloidal crystal | self-healing | inverse opal | structural color | hydrogel

Structural colors, arising from intrinsic periodic nanostructures and resulting in the interaction of light with these photonic nanostructures, have attracted much interest because of the fascination associated with the display of various brilliant examples (1–6). The creatures displaying brilliant structural colors are prevalent in nature, and their life, including communication, shielding, and other biological functions, is closely linked with these structural colors (7). Researchers, marveling at these miracles, have devoted their work to bio-inspired structure colors materials. Structural color hydrogels are one of the most important examples and have been widely studied and used in switches (8, 9), optical devices (10, 11), sensing materials (12, 13), and wearable electronics (14), etc. (15–20). However, because the deterioration and accumulation of damage of these materials during applications are inevitable, to achieve next-generation materials for both fundamental research and practical applications, the creation of bio-inspired structural color materials with increased survivability is still necessary.

Coincidentally, for the purpose of increasing the survivability and lifetime of an organism, the function of self-healing that can spontaneously heal injury and recover functionality in creatures is ubiquitous in nature (21–25). Inspired by these creatures, researchers have developed numerous self-healing hydrogel materials that fuse together with their homogeneous hydrogels for various important applications (26–37). However, the fusion process of the self-healing hydrogels could also happen in their neighboring nanostructures; this would cause the destruction of the periodic photonic scaffolds. Therefore, a self-healing hydrogel with stable structural color has not yet been reported, and its construction remains a challenge.

In this paper, we present the desired self-healing structural color hydrogels by constructing them with a composite nanostructure, as indicated in Fig. 1. This nanostructure was composed of a methacrylated gelatin (GelMA) hydrogel inverse opal scaffold and a filler of glutaraldehyde cross-linked BSA hydrogel with enzyme additives of glucose oxidase (GOX) and catalase (CAT). The polymerized GelMA hydrogel scaffold in the composite materials could guarantee the stability of both the inverse opal structure and its resultant structural colors, whereas the protein hydrogel filler could impart the materials with self-healing capability through the reversible covalent attachment of the glutaraldehyde to lysine residues of BSA and the enzyme additives. As both the GelMA and protein hydrogels are derived from organisms, the composite materials had high biocompatibility and plasticity. It was demonstrated that a series of new structural color materials with one-dimensional (1D) linear microfiber, 2D pattern, and 3D photonic path structures could be developed by assembling and healing the composite structural color hydrogel elements. These features make our self-healing structural color hydrogels highly promising for different applications, such as counterfeit prevention, integrated optics, and biomedical engineering.

Results and Discussion

In a typical experiment, the GelMA hydrogel inverse opal scaffolds were fabricated by replicating silica colloidal crystal templates. These colloidal crystal templates were prepared by the self-assembly of silica nanoparticles in silica capillaries or on glass slides, which closely packed and finally formed an ordered structure during dehydration (Fig. 2*A*). This ordered packing of the nanoparticles endowed the colloidal crystals with interconnected nanopores throughout the templates, which enabled infiltration of the GelMA pregel solution. After the pregel solution penetrated the nanopores and filled all of the voids of the templates by capillary action, the solution was polymerized to form a hydrogel by UV light. Finally, the inverse opal scaffolds were obtained by etching the silica nanoparticles, leaving an inverse opal GelMA hydrogel scaffold (Fig. 2*B*). This kind of scaffold displays various brilliant structure colors (Fig. S1), which is an important feature of the materials.

To impart to the structural color hydrogel the capability of self-healing, the glutaraldehyde cross-linked BSA hydrogel with enzyme additives of GOX and CAT was filled into the inverse opal scaffold. In this process, the pregel was first prepared with a

Significance

Structural color hydrogels have been widely studied and used in different applications, such as in switches, optical devices, etc. However, because the deterioration and accumulation of damage of these materials are inevitable during applications, the creation of bio-inspired structure color materials with increased survivability is still desired for both fundamental research and practical applications. In this study, inspired by creatures in nature with spontaneous healing from injury and recovering of functionality, we demonstrated a self-healing structural color hydrogel by filling a healable protein hydrogel into an inverse opal scaffold. A series of new structural color materials with 1D linear microfiber, 2D pattern, and 3D photonic path structures could be constructed by assembling and healing the composite structural color hydrogel elements.

Author contributions: Y.Z. designed research; F.F. and Z.C. performed research; F.F., Z.C., Z.Z., H.W., L.S., Z.G., and Y.Z. analyzed data; F.F. and Y.Z. wrote the paper; Z.Z. contributed to scientific discussion; and H.W. and L.S. contributed to scientific discussion of the article.

The authors declare no conflict of interest.

This article is a PNAS Direct Submission.

[1]F.F. and Z.C. contributed equally to this work.

[2]To whom correspondence should be addressed. Email: yjzhao@seu.edu.cn.

This article contains supporting information online at www.pnas.org/lookup/suppl/doi:10.1073/pnas.1703616114/-/DCSupplemental.

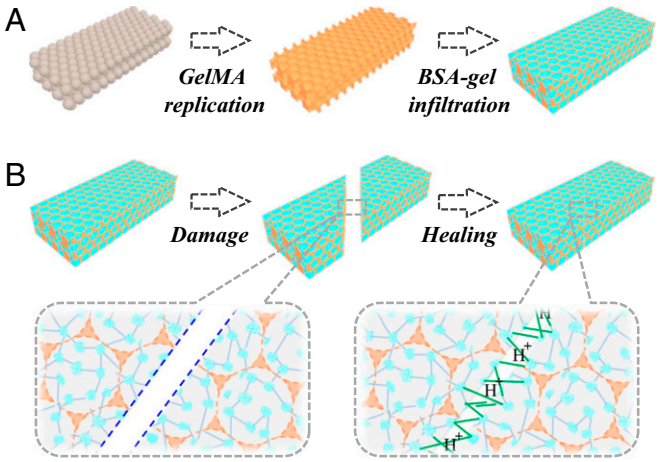

Fig. 1. Schematic diagram of the self-healing structural color hydrogel. (*A*) Fabrication of the self-healing structural color hydrogel. It was composed of a GelMA hydrogel inverse opal scaffold and a filler of glutaraldehyde cross-linked BSA hydrogel with GOX and CAT additives. (*B*) Self-healing process of the structural color hydrogel.

protein concentration of 13.5 wt% (GOX, CAT, and BSA for 0.2%, 0.8%, and 12.5%, respectively). The concentration of glutaraldehyde was 0.5 wt%, and the pH of the solution was adjusted to 7.0. To fully fill the protein hydrogel into the nanopores of the inverse opal, the structure color hydrogels should be dehydrated and then immersed in the pregel solution in a vacuum environment. After these steps, the structure color hydrogels were transferred to a closed environment with a certain humidity for the polymerization of the infiltrated pregel in the inverse opals (Fig. 2*C*). Finally, a hybrid inverse opal hydrogel with brilliant structure color was achieved.

The formation of the structural colors of the hydrogels was ascribed to their orderly arranged nanostructure, which imparts to the inverse opal hydrogel and its derived hybrid hydrogel a unique photonic band gap (PBG). This PBG leads light with certain wavelengths or frequencies to be located in and reflected instead of propagating through the materials. As a result, the colloidal crystal templates and the inverse opal scaffold, together with the hybrid hydrogel, all showed vivid colors and possessed characteristic reflection peaks. Under normal incidence, the main reflection peak position λ of these materials can be estimated by Bragg's equation, $\lambda = 2d_{111}n_{average}$, where d_{111} is the interplanar distance of the (111) diffracting planes, and $n_{average}$ refers to the average refractive index of the materials. Although the infiltration of the protein hydrogel into the inverse opal could increase the $n_{average}$ of the hybrid material, the d_{111}-related scaffold has also shrunk during the polymerization of the filler, and thus the structural color and the reflection peak of the hybrid material have blue shifted (Fig. S1). In addition, by using different sizes of silica nanoparticles for the colloidal crystal templates, a series of GelMA hydrogel inverse opals and resultant hybrid hydrogels with different diffraction peaks and structural colors could also be obtained (Fig. 2*D* and Fig. S2).

In the GelMA and proteins hybrid hydrogel system, the feature of reversible imine covalent attachment of the glutaraldehyde to lysine residues of BSA, GOX, and CAT proteins imparts to the inverse opal filler protein hydrogel the self-healing function, which uses GOX and CAT to adjust the pH of the system by adding extra traces of glucose (Fig. S3). In this process, GOX assists the glucose to be oxidized to gluconolactone, which is then hydrolyzed to gluconic acid to decrease the pH value of the protein hydrogel. The by-product H_2O_2 of the glucose oxidation will decompose into H_2O and O_2 by the CAT enzyme to avoid the imine bonds being oxidized and to support the cyclic reaction of glucose oxidation. Finally, with the regulation of pH, the imine bonds provide the opportunity to heal the protein hydrogel. As a benefit from the reversible binding of the inverse opal filler protein hydrogel, the GelMA and proteins hybrid structural color hydrogel system would also be imparted with a self-healing function.

To investigate the self-healing property of GelMA and the proteins' hybrid structural color hydrogel system, hybrid hydrogel microfibers with the same inverse opal nanostructures and composite protein materials were fabricated and cut into segments. Then, the segments of the structural color hydrogels were brought together slightly to ensure that their surfaces were in full contact. It was found that by simply connecting two of the segments, they could not adhere to each other and remained independent. However, with the addition of glucose, the two segments could adhere tightly to each other and form an integrated microfiber (Fig. 3*A*). Although the repaired traces could not be hidden and the reflection peak width at the fracture increased slightly (Fig. S4), the self-healing structural color microfiber maintained its vivid structural color through the whole body. In addition, the self-healing microfibers show elasticity as good as their original elasticity. Thus, the enzyme-mediated hybrid structural color hydrogel exhibits excellent self-healing properties with high recovery and reversibility.

It is noteworthy that our strategy could even heal the microfiber segments with different structural colors. To demonstrate this, hybrid hydrogel microfiber segments with blue, green, and red structural colors were assembled together. The joints of these microfiber segments were simply treated with glucose. It was found that although having different structural colors, neighbor segments could still adhere together tightly and form an integrated microfiber. The combined microfiber inherited the multiplex structural colors of each segment and preserved the good elasticity of the original microfibers (Fig. 3*B*). This indicated that the enzyme-mediated hybrid structural color hydrogel was suitable for different kinds of inverse opal scaffolds with different nanometer aperture sizes. Therefore, a new assembly strategy for the construction of a multiplex structural color hydrogel was developed.

To demonstrate the versatility of the self-healing structural color hydrogels in assembling other shapes besides cylindrical, three pieces of different hybrid hydrogel films were used for structural color pattern construction. By adding glucose to the intersection line, these films were stitched together to form an

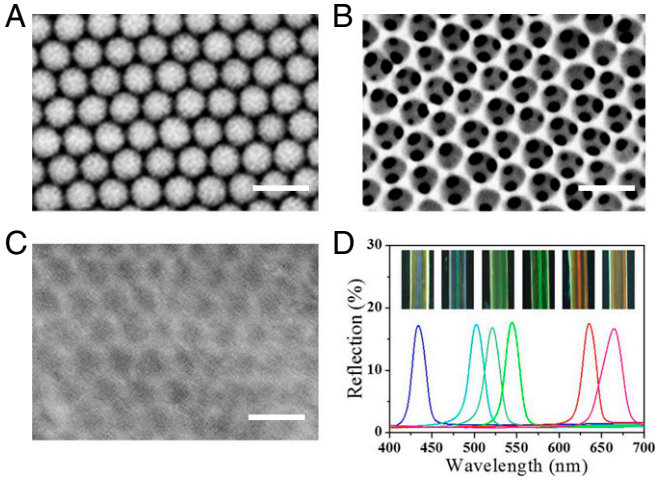

Fig. 2. (*A–C*) SEM images of (*A*) colloidal crystal template, (*B*) inverse opal scaffold, and (*C*) hybrid self-healing hydrogel surface. (Scale bars: 500 nm.) (*D*) Optical images and absolute reflection spectra of six kinds of hybrid self-healing hydrogel microfibers.

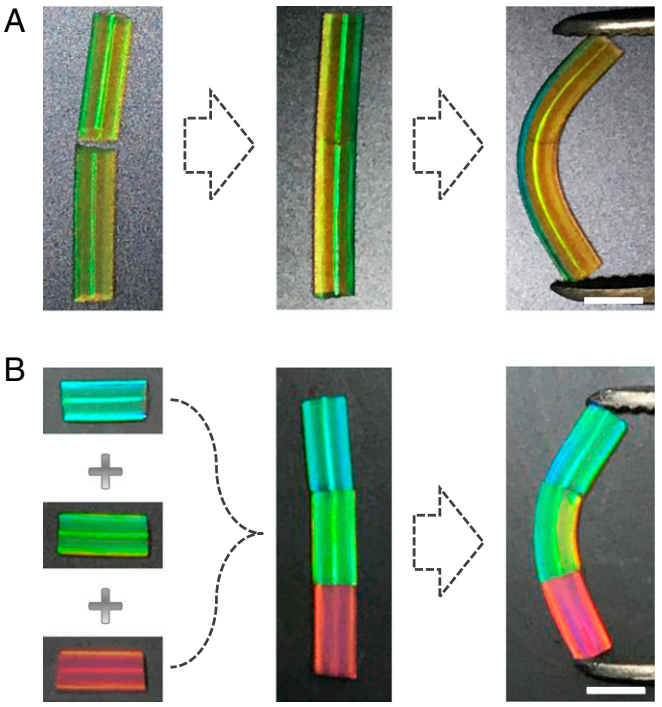

Fig. 3. Optical images of the self-healing process of the structural color microfibers. (*A*) Optical images of the self-healing process of two segments of the structural color hydrogel microfiber. (*B*) Optical images of the self-healing process of three different structural color hydrogel segments. (Scale bars: 2 mm.)

indexed pattern of an integrated film with blue, green, and red structural colors (Fig. 4*A*). To investigate the practical value of the self-healing hybrid hydrogel materials, a tensile test was performed to quantitatively evaluate the mechanical stability of the repaired sample. It was found that the self-healing film could keep its integrated structures not only in the assembled units but also in the repaired section (Fig. 4*B*). Thus, the self-healing structural color film is sufficiently flexible to resist an external tensile force (Fig. S5). In each assembled unit, it could be observed that all of them showed an equal ratio of stretching with the whole film, which caused the blue shift of their structural colors. These colors' blue shift should ascribe to the gradual decreasing of the interplanar distance d_{111} of the (111) diffracting planes during the stretching of the inverse opal materials. In addition to the simple indexed pattern of structural colors, a much more complex 2D pattern, such as Chinese Taiji (Fig. 4*C*), could also be constructed by using the same self-healing assembly strategy.

Besides the 2D patterns, the self-healing assembly strategy could also be used for the development of 3D structural color materials that have potential values in the areas of art creation, counterfeit prevention, and 3D integrated optics, etc. To demonstrate these concepts, a GelMA and proteins hybrid yellow structural color hydrogel film was cut into pieces of different sizes. These pieces were stacked together from large to small (Fig. 5*A*). Because of the complete porous inverse opal structure of these pieces, the filler self-healing protein hydrogels in the inverse opal scaffolds from the surface of the pieces could touch each other. Thus, these pieces could form an integrated 3D pyramid structure by a self-healing assembly strategy (Fig. 5*B*).

With the same method, we could also construct 3D structural color objects in a hydrogel block. In this process, hybrid blue structural color hydrogel pieces with different 2D green triangle patterns were first prepared by using the above process. Then, the pieces were stacked together and treated with glucose (Fig. 5*C*). Finally, a transparent blue hydrogel block containing a 3D triangle-stacked structural color object was generated (Fig. 5*D*). By designing the objects with more complex shapes and structural colors, advanced counterfeit prevention tags could be achieved. By using slender structural color microfibers instead of the triangle pattern, a 3D integrated photonic path could be

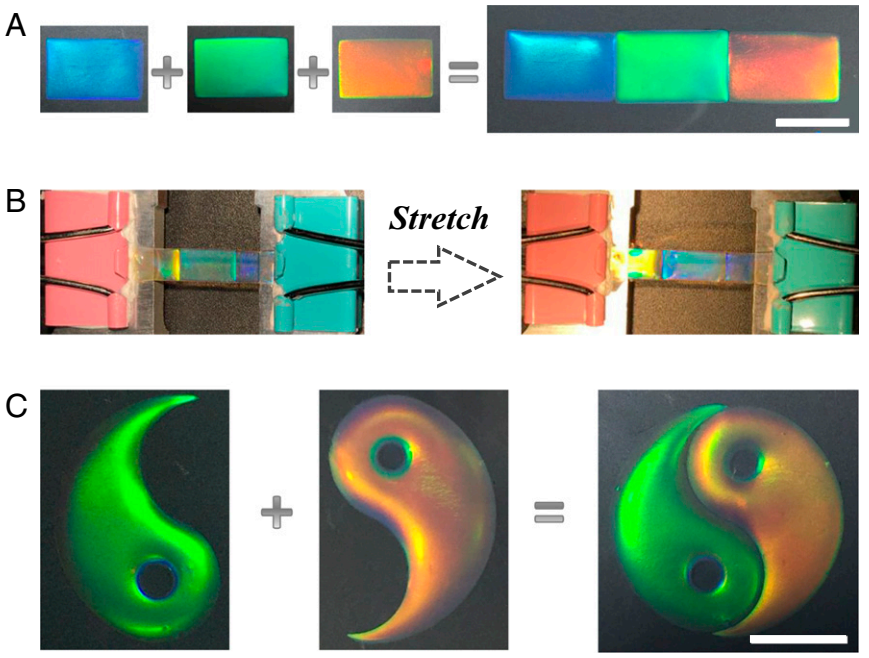

Fig. 4. Optical images of the self-healing process of the structural color films. (*A*) The construction process of a structural color hydrogel film by using three pieces of hybrid hydrogel with different structural colors. (*B*) The self-healing structural color hydrogel film from *A* showed good flexibility to resist external tensile force. (*C*) Optical image of a Chinese Taiji pattern assembled by the self-healing structural color hydrogel. (Scale bars for *A* and *C*: 5 mm.)

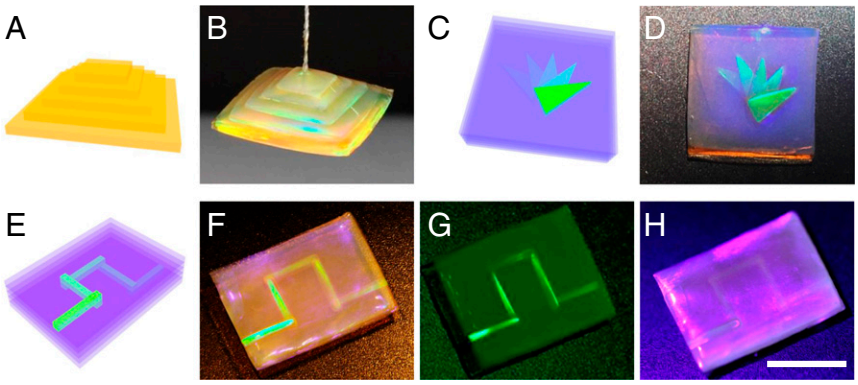

Fig. 5. Construction of 3D structural color objects. (*A* and *B*) Schematic diagram and optical image of a yellow pyramid-structured structural color hydrogel. The hydrogel had an integrated structure and could be hung in the air in *B*. (*C* and *D*) Schematic diagram and optical image of a blue hydrogel block with a 3D triangle stacked green object inside. (*E*–*H*) Schematic diagram and optical images of the 3D integrated photonic paths in a hydrogel block. The images were taken under natural light (*F*), 550 nm monochromatic light (*G*), and 450 nm monochromatic light (*H*), respectively. (Scale bars: 5 mm.)

developed in the hydrogel block (Fig. 5 *E* and *F*). Because of the existence of the PBGs in the hydrogel block and its encapsulated photonic paths, the hybrid hydrogel could show excited 3D green or invisible optical paths under green or blue light irradiation, respectively (Fig. 5 *G* and *H*). This implies that the materials could be used as new carriers for a 3D optical waveguide or optical communication.

As both the GelMA hydrogel inverse opal scaffold and the filler of the protein hydrogel were derived from organisms, the self-healing structural color hybrid hydrogels should have the same high biocompatibility. To demonstrate this, the hybrid hydrogels before and after self-healing were all used for a hepatocellular carcinoma (HepG2) cell culture, respectively. The inverse opal GelMA hydrogel scaffold was also cultured with cells for the control group. It was found that the HepG2 cells could adhere and grow on the surface of the hybrid hydrogels irrespective of the repair process. These cells formed tight cell–cell connections both on the hybrid hydrogel film and on the healing section of the film after 24 h culture, as shown in Fig. 6 *A*–*D* and Fig. S6. The cell viabilities on the structural color hybrid hydrogels before and after self-healing, as well as on the commercial multiwell and on the inverse opal GelMA hydrogel scaffold, were also investigated quantitatively by using 3-(4, 5-dimethylthiazol-2-yl)-2,5-diphenyltetrazolium bromide (MTT) assays, as presented in Fig. 6*E*. It could be observed that the viability of the HepG2 cells shows no obvious differences on these hydrogel substrates. Thus, the self-healing hybrid hydrogels were suitable for cell culture and reproduction. It is noteworthy that in many cases tissue engineering required hydrogels have no self-healing function, which greatly limits their application. However, with our strategy, both non- and self-healing hydrogels could be combined as a hybrid together through cross-linking nanoscaffolds, and the resultant hydrogels could be endowed with the self-healing function to remedy the restrictions of the hydrogel biomaterials in biomedical applications.

Conclusion

In summary, we have developed self-healing structural color hydrogels with a GelMA inverse opal scaffold and BSA protein filler with GOX and CAT enzyme additives. The GelMA scaffold in the hybrid hydrogels guaranteed the stability of the inverse opal structure and the resultant structural colors, whereas the protein filler could impart the hydrogels' self-healing capability through the reversible covalent attachment of the glutaraldehyde to lysine residues of proteins. We have demonstrated that a series of unprecedented structural color materials with 1D linear structures, 2D patterns, and 3D counterfeit-prevention objects and photonic path structures could be created by assembling and healing the hybrid hydrogel elements. In addition, the biocompatibility and biological applicability of the GelMA and proteins hybrid structural color hydrogels were also demonstrated. These features of the self-healing structural color hydrogels indicated their versatile values in different areas.

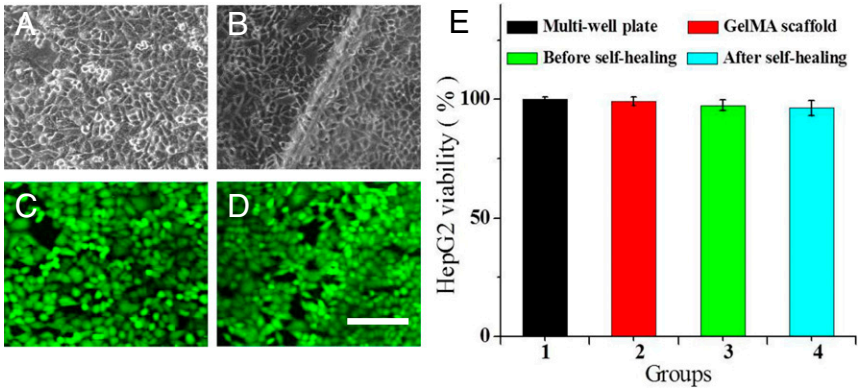

Fig. 6. (*A*–*D*) CLSM images of the HepG2 cells cultured on hybrid hydrogels before (*A* and *C*) and after (*B* and *D*) self-healing. *A* and *B* are the bright-field microscopy images, and *C* and *D* are the calcein-AM fluorescent images. (Scale bar: 100 μm.) (*E*) Results of the HepG2 cell MTT assays cultured on different hydrogels for 24 h.

Methods

Materials. Eight kinds of SiO_2 nanoparticles with sizes 200 nm, 210 nm, 230 nm, 250 nm, 270 nm, 290 nm, 300 nm, and 320 nm were purchased from Nanjing Dongjian Biological Technology Co., Ltd. The GelMA hydrogel was self-prepared. Gelatin (from porcine skin), methacrylic anhydride, and MTT were purchased from Sigma Aldrich. Calcein-AM (molecular probe) was purchased from Life Technologies, and glutaraldehyde was derived from Aladdin. BSA, GOX, and CAT were acquired from Sigma Aldrich. Cellulose dialysis membranes [molecular weight cutoff (MWCO) = 8,000–14,000] were acquired from Shanghai Yuanye Biotechnology Corporation. HepG2 cells were from the Institute of Biochemistry and Cell Biology, the Chinese Academy of Sciences, Shanghai, China. Dulbecco's modified Eagle's medium (DMEM) and FBS were purchased from HyClone. Penicillin–streptomycin was obtained from Gibco. Water used in all experiments was purified using a Milli-Q Plus 185 water purification system (Millipore) with resistivity higher than 18 MΩ•cm.

Preparation of Inverse Opal Scaffold. The inverse opal scaffolds were fabricated using a sacrificial template method. The colloidal crystal templates were obtained at invariant temperature and humidity by a vertical deposition method. In brief, the colloidal crystal templates were prepared with the self-assembly of silica nanoparticles in silica capillaries or on glass slides. The SiO_2 nanoparticles (50 wt%) with a variety of particle sizes (200 nm, 210 nm, 230 nm, 250 nm, 270 nm, 290 nm, 300 nm, and 320 nm) were dispersed in water, showing a good monodispersity. For the preparation of colloidal crystal fiber templates, the SiO_2 solution was injected into silica tubes (d = 1.56 mm) and formed an ordered fiber cluster structure during the dehydration procedure at 40 °C for 15 d. Then the fiber templates were calcined at 750 °C for 5 h to improve their mechanical strength. Finally, the silica tubes were removed and the free templates were obtained. The colloidal crystal film templates (with thickness of about 0.5 mm) were also prepared to obtain different patterns under the same condition. The silica nanoparticles self-assembled on glass slides with a silica solution (ethyl alcohol) concentration of 20 wt% at 4 °C for 3 h, and then the glass were calcined at 450 °C for 5 h to improve their mechanical strength. The inverse opal structural color hydrogels scaffold was obtained based on these colloidal crystal templates. The GelMA pregel solution (0.2 g/mL) was infiltrated into the silica templates by capillary force, and the solution was polymerized to form a hydrogel (with refractive index about 1.387) by exposure to UV light. Finally, the inverse opal scaffold was obtained by etching (4 wt% hydrofluoric acid) the silica nanoparticles, leaving an inverse opal GelMA hydrogel scaffold. These inverse opal scaffolds with different patterns could also be obtained by exposure to UV light with mask templates.

Preparation of Bio-Inspired Self-Healing Structural Color Hydrogels. The bio-inspired self-healing structural color hydrogels were prepared based on the enzyme additives of the GOX and CAT. The glutaraldehyde (0.5 wt%) cross-linked BSA (12.5 wt%) hydrogel with GOX (0.2 wt%) and CAT (0.8 wt%) was filled into the inverse opal scaffold. In this process, the pH of the pregel solution was adjusted to 7.0. The inverse opal scaffold was dehydrated for 2 h at 35 °C and quickly filled with the pregel solution (with refractive index about 1.352) in a vacuum environment for 20 min. After these steps, the structure color hydrogels were transferred into a closed environment with a certain humidity at 4 °C for another 3 h for polymerization of the infiltrated pregel in the inverse opals. Finally, the hybrid structural color hydrogels with good visibility and brilliant structural colors were prepared. In addition, by using different sizes of silica nanoparticles, a series of hybrid hydrogels with different diffraction peaks and structural colors could also be obtained. The optical microscopy images of the colloidal crystal templates, inverse opal scaffold, and hybrid hydrogels were obtained under the same conditions by a digital camera (Canon5D Mark II). The reflection spectra of these samples were recorded at a fixed glancing angle, using an optical microscope equipped with a fiber-optic spectrometer (Ocean Optics; USB2000-FLG).

The Construction Process of Structured Structural Color Hydrogels. The self-healing property of cross-linked protein hydrogel systems was investigated by cutting the hybrid structural color hydrogels into two segments. Then, two segments of the hybrid structural color hydrogels were brought together slightly to ensure the two surfaces were fully contacted and stimulated with external glucose (0.1 mg) for 3 h under a closed condition at 4 °C. Finally, the enzyme-mediated hybrid structural color hydrogels, exhibiting excellent self-healing properties, were prepared. In another experiment, three kinds of hybrid hydrogel fibers with different structure colors were assembled together under the same conditions. The 2D pattern and 3D photonic path structures could also be developed by assembling and healing the composite structural color hydrogel elements. Obtained by using mask templates of UV light, these inverse opal scaffolds in different shapes were first dehydrated for 2 h at 35 °C and quickly filled with the prepared solution in a vacuum environment for 20 min. Then, the 2D pattern and 3D photonic path structures could also be assembled together with an external glucose for 3 h under a closed condition at 4 °C. The optical microscopy images of the samples were obtained under the same conditions by a digital camera (Canon5D Mark II).

Cell Culture. Cells were regularly cultured and passaged with DMEM supplemented with 10% FBS and 1% penicillin–streptomycin in a humidified incubator at 37 °C with 5% CO_2. The structural color hydrogels were first disinfected by exposure to UV light for 2 h and rinsed with sterile PBS solution three times before cell culture. Then the HepG2 cells, cultured on the surface of the structure color hydrogels, were treated in traditional ways. The cells were seeded on the surface of hydrogel films (1 cm^2) in a six-well tissue culture plate (2×10^5 cells per well) for 24 h. The viability of HepG2 cells cultured in different structural color hydrogels was analyzed. Briefly, cells were first cultured on the surface of the structure color hydrogel films for 24 h, then MTT/PBS solution (5 μg/mL) was added, and the cells were incubated for another 4 h. Then the cell viability was quantified by the MTT assays according to the manufacturer's instructions. To test different cell viabilities under the same conditions, the cells cultured on the tissue culture plate were set as control experiments. The mean value and SD of five paralleled assays for each sample were recorded. The morphology of cells was also observed. After being cultured on the surface of the structure color hydrogel films for 24 h, the cells were stained with calcein AM (2 μg/mL, 2 mL per well) for 20 min at 37 °C, followed by being rinsed twice with PBS and fixed with glutaraldehyde (2.5%, 2 mL per well) for 6 h at 4 °C. Finally, the cells were observed using an inverted fluorescence microscope.

Characterization. Reflection spectra were obtained at a fixed glancing angle, using an optical microscope equipped with a fiber-optic spectrometer (Ocean Optics; USB2000-FLG). SEM images of samples were taken by a scanning electron microscope (Hitachi S-3000N). Microscopy images of the samples were obtained with an optical microscope (Olympus BX51) equipped with a CCD camera (Media Cybernetics Evolution MP5.0) and a digital camera (Canon5D Mark II). The stiffness of the hydrogel materials was characterized by Single Column Table Top Systems (5943; Instron).

ACKNOWLEDGMENTS. This work was supported by the National Science Foundation of China (Grants 21473029 and 51522302), the NSAF Foundation of China (Grant U1530260), the National Science Foundation of Jiangsu (Grant BK20140028), the Program for New Century Excellent Talents in University, the Scientific Research Foundation of Southeast University, and the Scientific Research Foundation of the Graduate School of Southeast University (Grant YBJJ1671).

1. Ge J, Yin Y (2011) Responsive photonic crystals. *Angew Chem Int Ed Engl* 50: 1492–1522.
2. Zhao Y, Xie Z, Gu H, Zhu C, Gu Z (2012) Bio-inspired variable structural color materials. *Chem Soc Rev* 41:3297–3317.
3. Ye B, et al. (2014) Photonic crystal microcapsules for label-free multiplex detection. *Adv Mater* 26:3270–3274.
4. Zhao Y, Shang L, Cheng Y, Gu Z (2014) Spherical colloidal photonic crystals. *Acc Chem Res* 47:3632–3642.
5. Lee HS, et al. (2014) Magnetoresponsive discoidal photonic crystals toward active color pigments. *Adv Mater* 26:5801–5807.
6. Qin M, et al. (2016) A rainbow structural-color chip for multisaccharide recognition. *Angew Chem Int Ed Engl* 55:6911–6914.
7. Shang LR, Gu ZZ, Zhao YJ (2016) Structural color materials in evolution. *Mater Today* 19:420–421.
8. Hou J, et al. (2015) Hydrophilic-hydrophobic patterned molecularly imprinted photonic crystal sensors for high-sensitive colorimetric detection of tetracycline. *Small* 11: 2738–2742.
9. Gu H, et al. (2013) Tailoring colloidal photonic crystals with wide viewing angles. *Small* 9:2266–2271.
10. Hou J, et al. (2014) Bio-inspired photonic-crystal microchip for fluorescent ultratrace detection. *Angew Chem Int Ed Engl* 53:5791–5795.
11. Zhang P, et al. (2016) Superspreading on immersed gel surfaces for the confined synthesis of thin polymer films. *Angew Chem Int Ed Engl* 55:3615–3619.
12. Kim SH, Shim JW, Yang SM (2011) Microfluidic multicolor encoding of microspheres with nanoscopic surface complexity for multiplex immunoassays. *Angew Chem Int Ed Engl* 50:1171–1174.
13. Liu CH, et al. (2016) Tunable structural color surfaces with visually self-reporting wettability. *Adv Funct Mater* 26:7937–7942.

14. Su B, Tian Y, Jiang L (2016) Bioinspired interfaces with superwettability: From materials to chemistry. *J Am Chem Soc* 138:1727–1748.
15. Yu L, Liu X, Yuan W, Brown LJ, Wang D (2015) Confined flocculation of ionic pollutants by poly (L-dopa)-based polyelectrolyte complexes in hydrogel beads for three-dimensional, quantitative, efficient water decontamination. *Langmuir* 31:6351–6366.
16. Shang L, et al. (2015) Photonic crystal microbubbles as suspension barcodes. *J Am Chem Soc* 137:15533–15539.
17. Wang M, He L, Xu W, Wang X, Yin Y (2015) Magnetic assembly and field-tuning of ellipsoidal-nanoparticle-based colloidal photonic crystals. *Angew Chem Int Ed Engl* 54:7077–7081.
18. Zhao Y, et al. (2013) Bioinspired multifunctional Janus particles for droplet manipulation. *J Am Chem Soc* 135:54–57.
19. Bai S, Nguyen TL, Mulvaney P, Wang D (2010) Using hydrogels to accommodate hydrophobic nanoparticles in aqueous media via solvent exchange. *Adv Mater* 22: 3247–3250.
20. Kim SH, Shum HC, Kim JW, Cho JC, Weitz DA (2011) Multiple polymersomes for programmed release of multiple components. *J Am Chem Soc* 133:15165–15171.
21. Cordier P, Tournilhac F, Soulié-Ziakovic C, Leibler L (2008) Self-healing and thermoreversible rubber from supramolecular assembly. *Nature* 451:977–980.
22. Griffin DR, Weaver WM, Scumpia PO, Di Carlo D, Segura T (2015) Accelerated wound healing by injectable microporous gel scaffolds assembled from annealed building blocks. *Nat Mater* 14:737–744.
23. Li CH, et al. (2016) A highly stretchable autonomous self-healing elastomer. *Nat Chem* 8:618–624.
24. Deng GH, Tang CM, Li FY, Jiang HF, Chen YM (2010) Covalent cross-linked polymer gels with reversible sol-gel transition and self-healing properties. *Macromolecules* 43: 1191–1194.
25. Cheng Y, et al. (2014) Bioinspired multicompartmental microfibers from microfluidics. *Adv Mater* 26:5184–5190.
26. Xing LX, et al. (2016) Self-healable polymer nanocomposites capable of simultaneously recovering multiple functionalities. *Adv Funct Mater* 26:3524–3531.
27. Shang L, et al. (2017) Bioinspired multifunctional spindle-knotted microfibers from microfluidics. *Small* 13:201600286.
28. Liu X, Wang S (2014) Three-dimensional nano-biointerface as a new platform for guiding cell fate. *Chem Soc Rev* 43:2385–2401.
29. Wang SG, et al. (2016) Phase-changeable and bubble-releasing implants for highly efficient HIFU-responsive tumor surgery and chemotherapy. *J Mater Chem B Mater Biol Med* 4:7368–7378.
30. Gao Y, et al. (2014) Enzymetically regulating the self-healing of protein hydrogels with high healing efficiency. *Angew Chem Int Ed Engl* 53:9343–9346.
31. Cai G, et al. (2016) Extremely stretchable strain sensors based on conductive self-healing dynamic cross-links hydrogels for human-motion detection. *Adv Sci* 4:1600190.
32. Zhao X, Zhang MY, Guo BL, Ma PX (2016) Mussel-inspired injectable supramolecular and covalent bonds crosslinked hydrogels with rapid self-healing and recovery via a facile approach under metal-free conditions. *J Mater Chem B Mater Biol Med* 4:6644–6651.
33. Huang W, et al. (2016) Strong and rapidly self-healing hydrogels: Potential hemostatic materials. *Adv Healthc Mater* 5:2813–2822.
34. Dong R, Zhao X, Guo B, Ma PX (2016) Self-healing conductive injectable hydrogels with antibacterial activity as cell delivery carrier for cardiac cell therapy. *ACS Appl Mater Interfaces* 8:17138–17150.
35. Zeng Q, et al. (2016) Self-healing elastin-bioglass hydrogels. *Biomacromolecules* 17: 2619–2625.
36. Wang S, et al. (2011) Highly efficient capture of circulating tumor cells by using nanostructured silicon substrates with integrated chaotic micromixers. *Angew Chem Int Ed Engl* 50:3084–3088.
37. Zhu Y, Xuan H, Ren J, Ge L (2015) Self-healing multilayer polyelectrolyte composite film with chitosan and poly(acrylic acid). *Soft Matter* 11:8452–8459.